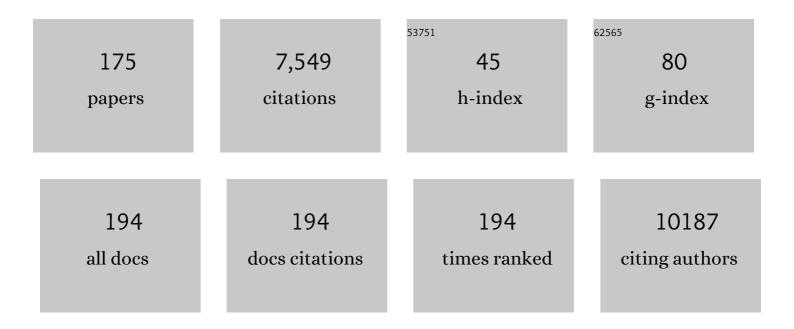
List of Publications by Year in descending order

Source: https://exaly.com/author-pdf/2502108/publications.pdf Version: 2024-02-01



#	Article	IF	CITATIONS
1	Solar hydrogen generation from seawater with a modified BiVO4 photoanode. Energy and Environmental Science, 2011, 4, 4046.	15.6	564
2	Robust Hollow Spheres Consisting of Alternating Titania Nanosheets and Graphene Nanosheets with High Photocatalytic Activity for CO ₂ Conversion into Renewable Fuels. Advanced Functional Materials, 2012, 22, 1215-1221.	7.8	373
3	Ultrathin, Single-Crystal WO ₃ Nanosheets by Two-Dimensional Oriented Attachment toward Enhanced Photocatalystic Reduction of CO ₂ into Hydrocarbon Fuels under Visible Light. ACS Applied Materials & Interfaces, 2012, 4, 3372-3377.	4.0	332
4	Structure and chemical composition of supported Pt–Sn electrocatalysts for ethanol oxidation. Electrochimica Acta, 2005, 50, 5384-5389.	2.6	260
5	FT-IR study of the microstructure of NafionÂ $^{\odot}$ membrane. Journal of Membrane Science, 2004, 233, 39-44.	4.1	246
6	Novel synthesis of highly active Pt/C cathode electrocatalyst for direct methanol fuel cell. Chemical Communications, 2003, , 394-395.	2.2	226
7	Nanoporous gold as non-enzymatic sensor for hydrogen peroxide. Electrochimica Acta, 2011, 56, 4657-4662.	2.6	206
8	Inhibiting excessive acidification using zero-valent iron in anaerobic digestion of food waste at high organic load rates. Bioresource Technology, 2016, 211, 65-71.	4.8	143
9	Studies on performance degradation of a direct methanol fuel cell (DMFC) in life test. Physical Chemistry Chemical Physics, 2004, 6, 134.	1.3	135
10	In situ deposition of platinum nanoparticles on bacterial cellulose membranes and evaluation of PEM fuel cell performance. Electrochimica Acta, 2009, 54, 6300-6305.	2.6	127
11	Influence of electrode structure on the performance of a direct methanol fuel cell. Journal of Power Sources, 2002, 106, 364-369.	4.0	124
12	Design, implementation, and evaluation of an Internet of Things (IoT) network system for restaurant food waste management. Waste Management, 2018, 73, 26-38.	3.7	124
13	Comparative characterization of sewage sludge compost and soil: Heavy metal leaching characteristics. Journal of Hazardous Materials, 2016, 310, 1-10.	6.5	118
14	Environmental performance evaluation of different municipal solid waste management scenarios in China. Resources, Conservation and Recycling, 2017, 125, 98-106.	5.3	114
15	One-step growth of CoNi2S4 nanoribbons on carbon fibers as platinum-free counter electrodes for fiber-shaped dye-sensitized solar cells with high performance: Polymorph-dependent conversion efficiency. Nano Energy, 2015, 11, 697-703.	8.2	108
16	The degradation study of Nafion/PTFE composite membrane in PEM fuel cell under accelerated stress tests. International Journal of Hydrogen Energy, 2014, 39, 14381-14390.	3.8	103
17	Study of sintered stainless steel fiber felt as gas diffusion backing in air-breathing DMFC. Journal of Power Sources, 2004, 133, 175-180.	4.0	102
18	Constructing a High-Efficiency MoO ₃ /Polyimide Hybrid Photocatalyst Based on Strong Interfacial Interaction. ACS Applied Materials & Interfaces, 2015, 7, 14628-14637.	4.0	97

#	Article	IF	CITATIONS
19	Dispersing Pt atoms onto nanoporous gold for high performance direct formic acid fuel cells. Chemical Science, 2014, 5, 403-409.	3.7	93
20	Haze insights and mitigation in China: An overview. Journal of Environmental Sciences, 2014, 26, 2-12.	3.2	91
21	High catalytic activity and stability of nickel sulfide and cobalt sulfide hierarchical nanospheres on the counter electrodes for dye-sensitized solar cells. Chemical Communications, 2014, 50, 4824-4826.	2.2	90
22	Enhanced photovoltaic performance of a dye-sensitized solar cell using graphene–TiO2 photoanode prepared by a novel in situ simultaneous reduction-hydrolysis technique. Nanoscale, 2013, 5, 3481.	2.8	89
23	Release of heavy metals during long-term land application of sewage sludge compost: Percolation leaching tests with repeated additions of compost. Chemosphere, 2017, 169, 271-280.	4.2	81
24	Atmosphere boundary layer height and its effect on air pollutants in Beijing during winter heavy pollution. Atmospheric Research, 2019, 215, 305-316.	1.8	79
25	High Performance Cross-Linked Poly(2-acrylamido-2-methylpropanesulfonic acid)-Based Proton Exchange Membranes for Fuel Cells. Macromolecules, 2010, 43, 6398-6405.	2.2	78
26	Greenhouse gas emissions from different municipal solid waste management scenarios in China: Based on carbon and energy flow analysis. Waste Management, 2017, 68, 653-661.	3.7	74
27	Effect of FeO addition on volatile fatty acids evolution on anaerobic digestion at high organic loading rates. Waste Management, 2018, 71, 719-727.	3.7	72
28	Direct N2H4/H2O2 Fuel Cells Powered by Nanoporous Gold Leaves. Scientific Reports, 2012, 2, 941.	1.6	67
29	Poisoning and regeneration of Pd catalyst in direct formic acid fuel cell. Electrochimica Acta, 2010, 55, 5024-5027.	2.6	66
30	<i>In Situ</i> Fabrication of Highly Conductive Metal Nanowire Networks with High Transmittance from Deep-Ultraviolet to Near-Infrared. ACS Nano, 2015, 9, 2502-2509.	7.3	65
31	Unique Zn-doped SnO2 nano-echinus with excellent electron transport and light harvesting properties as photoanode materials for high performance dye-sensitized solar cell. CrystEngComm, 2012, 14, 6462.	1.3	64
32	Characterization of naturally aged cement-solidified MSWI fly ash. Waste Management, 2018, 80, 101-111.	3.7	62
33	Novel method for comprehensive utilization of MSWI fly ash through co-reduction with red mud to prepare crude alloy and cleaned slag. Journal of Hazardous Materials, 2020, 384, 121315.	6.5	62
34	Primary and secondary sources of ambient formaldehyde in the Yangtze River Delta based on Ozone Mapping and Profiler Suite (OMPS) observations. Atmospheric Chemistry and Physics, 2019, 19, 6717-6736.	1.9	60
35	In situ grown vertically oriented CuInS2 nanosheets and their high catalytic activity as counter electrodes in dye-sensitized solar cells. Chemical Communications, 2013, 49, 2028.	2.2	59
36	Fabrication of hierarchically assembled microspheres consisting of nanoporous ZnO nanosheets for high-efficiency dye-sensitized solar cells. Journal of Materials Chemistry, 2012, 22, 14341.	6.7	57

#	Article	IF	CITATIONS
37	UNDERSTANDING FORCE CHAINS IN DENSE GRANULAR MATERIALS. International Journal of Modern Physics B, 2010, 24, 5743-5759.	1.0	56
38	Vertically building Zn2SnO4 nanowire arrays on stainless steel mesh toward fabrication of large-area, flexible dye-sensitized solar cells. Nanoscale, 2012, 4, 3490.	2.8	56
39	Greenhouse gas emissions from municipal solid waste with a high organic fraction under different management scenarios. Journal of Cleaner Production, 2017, 147, 451-457.	4.6	56
40	Comparison of long-term stability under natural ageing between cement solidified and chelator-stabilised MSWI fly ash. Environmental Pollution, 2019, 250, 68-78.	3.7	56
41	Direct immobilization of Pt–Ru alloy nanoparticles on nitrogen-doped carbon nanotubes with superior electrocatalytic performance. Journal of Power Sources, 2010, 195, 7578-7582.	4.0	54
42	Ultra-thin layer structured anodes for highly durable low-Pt direct formic acid fuel cells. Nano Research, 2014, 7, 1569-1580.	5.8	54
43	Tropospheric NO ₂ , SO ₂ , and HCHO over the East China Sea, using ship-based MAX-DOAS observations and comparison with OMI and OMPS satellite data. Atmospheric Chemistry and Physics, 2018, 18, 15387-15402.	1.9	49
44	Exploring the roles of zero-valent iron in two-stage food waste anaerobic digestion. Waste Management, 2020, 107, 91-100.	3.7	49
45	Effective and rapid electrochemical detection of hydrazine by nanoporous gold. Journal of Electroanalytical Chemistry, 2011, 661, 44-48.	1.9	48
46	Enhancing syntrophic associations among Clostridium butyricum, Syntrophomonas and two types of methanogen by zero valent iron in an anaerobic assay with a high organic loading. Bioresource Technology, 2018, 257, 181-191.	4.8	48
47	Porous, single crystalline titanium nitride nanoplates grown on carbon fibers: excellent counter electrodes for low-cost, high performance, fiber-shaped dye-sensitized solar cells. Chemical Communications, 2014, 50, 14321-14324.	2.2	45
48	Identifying the wintertime sources of volatile organic compounds (VOCs) from MAX-DOAS measured formaldehyde and glyoxal in Chongqing, southwest China. Science of the Total Environment, 2020, 715, 136258.	3.9	45
49	Performance Improvement in Direct Methanol Fuel Cell Cathode Using High Mesoporous Area Catalyst Support. Electrochemical and Solid-State Letters, 2005, 8, A12.	2.2	44
50	Investigating the performance of a greenhouse gas observatory in Hefei, China. Atmospheric Measurement Techniques, 2017, 10, 2627-2643.	1.2	44
51	Clay mineral compositions in surface sediments of the Ganges-Brahmaputra-Meghna river system of Bengal Basin, Bangladesh. Marine Geology, 2019, 412, 27-36.	0.9	44
52	Enhancing anaerobic digestion of high-pressure extruded food waste by inoculum optimization. Journal of Environmental Management, 2016, 166, 31-37.	3.8	42
53	Temporal and spatial patterns of sediment deposition in the northern South China Sea over the last 50,000 years. Palaeogeography, Palaeoclimatology, Palaeoecology, 2017, 465, 212-224.	1.0	41
54	Recovery of metals from municipal solid waste incineration fly ash and red mud via a co-reduction process. Resources, Conservation and Recycling, 2020, 154, 104600.	5.3	40

#	Article	IF	CITATIONS
55	Evaluating the impact of odors from the 1955 landfills in China using a bottom-up approach. Journal of Environmental Management, 2015, 164, 206-214.	3.8	39
56	Fiber dye-sensitized solar cells consisting of TiO2 nanowires arrays on Ti thread as photoanodes through a low-cost, scalable route. Journal of Materials Chemistry A, 2013, 1, 11790.	5.2	38
57	Porous ZnO nanosheet arrays constructed on weaved metal wire for flexible dye-sensitized solar cells. Nanoscale, 2013, 5, 5102.	2.8	38
58	Ship-based MAX-DOAS measurements of tropospheric NO ₂ , SO ₂ , and HCHO distribution along the Yangtze River. Atmospheric Chemistry and Physics, 2018, 18, 5931-5951.	1.9	38
59	Pd electroless plated Nafion® membrane for high concentration DMFCs. Journal of Membrane Science, 2005, 259, 27-33.	4.1	37
60	Full-circle range and microradian resolution angle measurement using the orthogonal mirror self-mixing interferometry. Optics Express, 2018, 26, 10371.	1.7	37
61	Influence of temperature on enhancement of volatile fatty acids fermentation from organic fraction of municipal solid waste: Synergism between food and paper components. Bioresource Technology, 2020, 304, 122980.	4.8	37
62	Toward separation at source: Evolution of Municipal Solid Waste management in China. Frontiers of Environmental Science and Engineering, 2020, 14, 1.	3.3	37
63	Effect of vanadium redox species on photoelectrochemical behavior of TiO2 and TiO2/WO3 photo-electrodes. Journal of Power Sources, 2012, 213, 78-82.	4.0	36
64	Vitamin E assisted polymer electrolyte fuel cells. Energy and Environmental Science, 2014, 7, 3362-3370.	15.6	35
65	Influence of Membrane Thickness on Membrane Degradation and Platinum Agglomeration under Long-term Open Circuit Voltage Conditions. Electrochimica Acta, 2015, 153, 254-262.	2.6	35
66	Preparation of Pt supported on WO3–C with enhanced catalytic activity by microwave-pyrolysis method. Journal of Power Sources, 2010, 195, 2633-2637.	4.0	34
67	Long-term characterization and resource potential evaluation of the digestate from food waste anaerobic digestion plants. Science of the Total Environment, 2021, 794, 148785.	3.9	34
68	Investigations of temporal and spatial distribution of precursors SO ₂ and NO ₂ vertical columns in the North China Plain using mobile DOAS. Atmospheric Chemistry and Physics, 2018, 18, 1535-1554.	1.9	32
69	Sedimentary responses to sea-level rise and Kuroshio Current intrusion since the Last Glacial Maximum: Grain size and clay mineral evidence from the northern South China Sea slope. Palaeogeography, Palaeoclimatology, Palaeoecology, 2016, 450, 111-121.	1.0	31
70	Dechlorination of hexachlorobenzene using lead–iron bimetallic particles. Chemosphere, 2013, 90, 2403-2407.	4.2	30
71	Mini art review for zero valent iron application in anaerobic digestion and technical bottlenecks. Science of the Total Environment, 2021, 791, 148415.	3.9	29
72	Heavy metal pollution in the soil around municipal solid waste incinerators and its health risks in China. Environmental Research, 2022, 203, 111871.	3.7	29

#	Article	IF	CITATIONS
73	Performance improvement of the open-cathode proton exchange membrane fuel cell by optimizing membrane electrode assemblies. International Journal of Hydrogen Energy, 2015, 40, 7159-7167.	3.8	27
74	Leaching characteristic of toxic trace elements in soils amended by sewage sludge compost: A comparison of field and laboratory investigations. Environmental Pollution, 2018, 237, 244-252.	3.7	27
75	High catalytic performance and stability of Pt/C using acetic acid functionalized carbon. Journal of Power Sources, 2009, 194, 683-689.	4.0	25
76	Effects of aerobic and anaerobic biological processes on leaching of heavy metals from soil amended with sewage sludge compost. Waste Management, 2016, 58, 324-334.	3.7	25
77	Development of a field system for measurement of tropospheric OH radical using laser-induced fluorescence technique. Optics Express, 2019, 27, A419.	1.7	25
78	Simulations of Bingham plastic flows with the multiple-relaxation-time lattice Boltzmann model. Science China: Physics, Mechanics and Astronomy, 2014, 57, 532-540.	2.0	24
79	Characterization of odorous charge and photochemical reactivity of VOC emissions from a full-scale food waste treatment plant in China. Journal of Environmental Sciences, 2015, 29, 34-44.	3.2	24
80	Development of a portable cavity ring down spectroscopy instrument for simultaneous, in situ measurement of NO3 and N2O5. Optics Express, 2018, 26, A433.	1.7	24
81	Direct NaBH4–H2O2 fuel cell based on nanoporous gold leaves. International Journal of Hydrogen Energy, 2013, 38, 10992-10997.	3.8	23
82	Versatile nanobead-scaffolded N-SnO2mesoporous microspheres: one-step synthesis and superb performance in dye-sensitized solar cell, gas sensor, and photocatalytic degradation of dye. Journal of Materials Chemistry A, 2013, 1, 524-531.	5.2	23
83	A new method to determine the aerosol optical properties from multiple-wavelength O ₄ absorptions by MAX-DOAS observation. Atmospheric Measurement Techniques, 2019, 12, 3289-3302.	1.2	23
84	Source-to-sink processes of fluvial sediments in the northern South China Sea: Constraints from river sediments in the coastal region of South China. Journal of Asian Earth Sciences, 2019, 185, 104020.	1.0	23
85	The performance improvement of membrane and electrode assembly in open-cathode proton exchange membrane fuel cell. International Journal of Hydrogen Energy, 2013, 38, 10978-10984.	3.8	22
86	Impact of cation selection on proton exchange membrane fuel cell performance with trimethylethyl amide, ethylpyridinium and ethylmethyl imidazolium ionic liquid carried by poly(vinylidene fluoride) membrane as electrolyte. Journal of Power Sources, 2014, 251, 432-438.	4.0	22
87	Targeted modification of organic components of municipal solid waste by short-term pre-aeration and its enhancement on anaerobic degradation in simulated landfill bioreactors. Bioresource Technology, 2016, 216, 250-259.	4.8	22
88	Leaching behavior and potential ecological risk of heavy metals in Southwestern China soils applied with sewage sludge compost under acid precipitation based on lysimeter trials. Chemosphere, 2020, 249, 126212.	4.2	22
89	MnO2 nanolayers on highly conductive TiO0.54N0.46 nanotubes for supercapacitor electrodes with high power density and cyclic stability. Physical Chemistry Chemical Physics, 2014, 16, 8521.	1.3	21
90	Staged fine-grained sediment supply from the Himalayas to the Bengal Fan in response to climate change over the past 50,000 years. Quaternary Science Reviews, 2019, 212, 164-177.	1.4	21

#	Article	IF	CITATIONS
91	HCB dechlorination combined with heavy metals immobilization in MSWI fly ash by using n-Al/CaO dispersion mixture. Journal of Hazardous Materials, 2020, 392, 122510.	6.5	21
92	An efficient and green approach to prepare hydrophilic imidazolium ionic liquids free of halide and its effect on oxygen reduction reaction of Pt/C catalyst. International Journal of Hydrogen Energy, 2012, 37, 13167-13177.	3.8	20
93	Curbing dioxin emissions from municipal solid waste incineration: China's action and global share. Journal of Hazardous Materials, 2022, 435, 129076.	6.5	20
94	Application of electrical resistivity tomography to evaluate the variation in moisture content of waste during 2Âmonths of degradation. Environmental Earth Sciences, 2013, 68, 57-67.	1.3	19
95	Effects of high-pressure extruding pretreatment on MSW upgrading and hydrolysis enhancement. Waste Management, 2016, 58, 81-89.	3.7	19
96	Short-term pre-aeration applied to the dry anaerobic digestion of MSW, with a focus on the spectroscopic characteristics of dissolved organic matter. Chemical Engineering Journal, 2017, 313, 1222-1232.	6.6	19
97	The Physical Clogging of the Landfill Leachate Collection System in China: Based on Filtration Test and Numerical Modelling. International Journal of Environmental Research and Public Health, 2018, 15, 318.	1.2	19
98	Phase distribution of PCDD/Fs in flue gas from municipal solid waste incinerator with ultra-low emission control in China. Chemosphere, 2021, 276, 130166.	4.2	19
99	Effects of temperature on pyrolysis products of oil sludge. Frontiers of Environmental Science and Engineering in China, 2008, 2, 8-14.	0.8	18
100	On-line analysis of algae in water by discrete three-dimensional fluorescence spectroscopy. Optics Express, 2018, 26, A251.	1.7	18
101	Study on baseline correction methods for the Fourier transform infrared spectra with different signal-to-noise ratios. Applied Optics, 2018, 57, 5794.	0.9	18
102	Effect of organic compositions of aerobically pretreated municipal solid waste on non-methane organic compound emissions during anaerobic degradation. Waste Management, 2012, 32, 1116-1121.	3.7	17
103	Long-term leaching behavior of phenol in cement/activated-carbon solidified/stabilized hazardous waste. Journal of Environmental Management, 2013, 115, 265-269.	3.8	17
104	Analysis of carbon-supported platinum through potential cycling and potential-static holding. International Journal of Hydrogen Energy, 2014, 39, 13725-13737.	3.8	17
105	A novel insight into the influence of thermal pretreatment temperature on the anaerobic digestion performance of floatable oil-recovered food waste: Intrinsic transformation of materials and microbial response. Bioresource Technology, 2019, 293, 122021.	4.8	17
106	Fe0 inhibits bio-foam generating in anaerobic digestion reactor under conditions of organic shock loading and re-startup. Waste Management, 2019, 92, 107-114.	3.7	17
107	Experimental study of proton exchange membrane fuel cells using Nafion 212 and Nafion 211 for portable application at ambient pressure and temperature conditions. International Journal of Hydrogen Energy, 2012, 37, 4673-4677.	3.8	16
108	Rapid synthesis of nitrogen-doped graphene by microwave heating for oxygen reduction reactions in alkaline electrolyte. Chinese Journal of Catalysis, 2014, 35, 509-513.	6.9	16

#	Article	IF	CITATIONS
109	Dechlorination of Hexachlorobenzene in Contaminated Soils Using a Nanometallic Al/CaO Dispersion Mixture: Optimization through Response Surface Methodology. International Journal of Environmental Research and Public Health, 2018, 15, 872.	1.2	16
110	Lidar vertical observation network and data assimilation reveal key processes driving the 3-D dynamic evolution of PM _{2.5} concentrations over the North China Plain. Atmospheric Chemistry and Physics, 2021, 21, 7023-7037.	1.9	16
111	Anthropogenic effect on heavy metal contents in surface sediments of the Bengal Basin river system, Bangladesh. Environmental Science and Pollution Research, 2020, 27, 19688-19702.	2.7	15
112	Using Lidar technology to assess regional air pollution and improve estimates of PM _{2.5} transport in the North China Plain. Environmental Research Letters, 2020, 15, 094071.	2.2	15
113	Intercomparison of NO x , SO2, O3, and aromatic hydrocarbons measured by a commercial DOAS system and traditional point monitoring techniques. Advances in Atmospheric Sciences, 2004, 21, 211-219.	1.9	14
114	Phytoplankton photosynthetic rate measurement using tunable pulsed light induced fluorescence kinetics. Optics Express, 2018, 26, A293.	1.7	14
115	Mechanism and dynamic evolution of leachate collection system clogging in MSW landfills in China. Waste Management, 2021, 120, 314-321.	3.7	14
116	Bacterial cellulose-assisted hydrothermal synthesis and catalytic performance of La2CuO4 nanofiber for methanol steam reforming. International Journal of Hydrogen Energy, 2013, 38, 10813-10818.	3.8	13
117	Impact assessment of intermediate soil cover on landfill stabilization by characterizing landfilled municipal solid waste. Journal of Environmental Management, 2013, 128, 259-265.	3.8	13
118	Solid phase polymerization of phenylenediamine toward a self-supported FeN _x /C catalyst with high oxygen reduction activity. Chemical Communications, 2015, 51, 16707-16709.	2.2	13
119	Fate of dioxins in a municipal solid waste incinerator with state-of-the-art air pollution control devices in China. Environmental Pollution, 2021, 289, 117798.	3.7	13
120	The maximum limiting performance improved counter electrode based on a porous fluorine doped tin oxide conductive framework for dye-sensitized solar cells. Nanoscale, 2013, 5, 4951.	2.8	12
121	Ammonium nitrate is a risk for environment: A case study of Beirut (Lebanon) chemical explosion and the effects on environment. Ecotoxicology and Environmental Safety, 2021, 210, 111834.	2.9	12
122	A quick and green approach to prepare [Rmim]OH and its application in hydrophilic ionic liquid synthesis. New Journal of Chemistry, 2011, 35, 1661.	1.4	11
123	Identification and characterization of odorous gas emission from a full-scale food waste anaerobic digestion plant in China. Environmental Monitoring and Assessment, 2015, 187, 624.	1.3	11
124	Geochemistry of core sediments along the Active Channel, northeastern Indian Ocean over the past 50,000†years: Sources and climatic implications. Palaeogeography, Palaeoclimatology, Palaeoecology, 2019, 521, 151-160.	1.0	11
125	Vertical profile of aerosols in the Himalayas revealed by lidar: New insights into their seasonal/diurnal patterns, sources, and transport. Environmental Pollution, 2021, 285, 117686.	3.7	11
126	Intermittent microwave synthesis of nanostructured Pt/TiN–graphene with high catalytic activity for methanol oxidation. International Journal of Hydrogen Energy, 2014, 39, 16036-16042.	3.8	10

#	Article	IF	CITATIONS
127	The effect of ISR on OFMSW during acidogenic fermentation for the production of AD precursor: kinetics and synergies. RSC Advances, 2019, 9, 18147-18156.	1.7	10
128	New archive of another significant potential sediment source in the South China Sea. Marine Geology, 2019, 410, 16-21.	0.9	10
129	Validation of Water Vapor Vertical Distributions Retrieved from MAX-DOAS over Beijing, China. Remote Sensing, 2020, 12, 3193.	1.8	10
130	The Determination of Aerosol Distribution by a No-Blind-Zone Scanning Lidar. Remote Sensing, 2020, 12, 626.	1.8	10
131	Quantifying variability, source, and transport of CO in the urban areas over the Himalayas and Tibetan Plateau. Atmospheric Chemistry and Physics, 2021, 21, 9201-9222.	1.9	10
132	Sea Level Change Controlled the Sedimentary Processes at the Makran Continental Margin Over the Past 13,000Âyr. Journal of Geophysical Research: Oceans, 2020, 125, e2019JC015703.	1.0	9
133	Insights into the effects of micro and nanoscale Fe0 on elimination of excessive acidification during anaerobic digestion of the organic fraction of municipal solid waste: Similarities and differences in reactor performance and syntrophic metabolism. Fuel, 2022, 320, 123923.	3.4	9
134	Study on Platinum and Copper Nanosheets Alloys Supported on Mesoporous Titanium Dioxide Doped with Carbon Black as Electrocatalysts in PEM Fuel Cells. Electroanalysis, 2012, 24, 699-706.	1.5	8
135	Design and synthesis of cation-functionalized ionic liquid for application as electrolyte in proton exchange membrane fuel cells. Journal of Materials Chemistry A, 2014, 2, 19275-19281.	5.2	8
136	Controllable electrophoresis deposition of TiO ₂ mesoporous spheres onto Ti threads as photoanodes for fiber-shaped dye-sensitized solar cells. RSC Advances, 2015, 5, 65005-65009.	1.7	8
137	Visualization of force networks in 2D dense granular materials. Frontiers of Architecture and Civil Engineering in China, 2010, 4, 109-115.	0.4	7
138	Cement-based solidification/stabilization of contaminated soils by nitrobenzene. Frontiers of Environmental Science and Engineering, 2012, 6, 437-443.	3.3	7
139	Aging of solidified/stabilized electrolytic manganese solid waste with accelerated carbonation and aging inhibition. Environmental Science and Pollution Research, 2016, 23, 24195-24204.	2.7	7
140	Development of a static test apparatus for evaluating the performance of three PM2.5 separators commonly used in China. Journal of Environmental Sciences, 2020, 87, 238-249.	3.2	7
141	An automated dynamic chamber system for exchange flux measurement of reactive nitrogen oxides (HONO and NOX) in farmland ecosystems of the Huaihe River Basin, China. Science of the Total Environment, 2020, 745, 140867.	3.9	7
142	Reconstruction of a leaking gas cloud from a passive FTIR scanning remote-sensing imaging system. Applied Optics, 2021, 60, 9396.	0.9	7
143	The influence of mesoscale eddies on sedimentary processes in the western South China Sea since 32 kyr BP. Marine Geology, 2021, 441, 106621.	0.9	7
144	Determining the Biodegradability of Leachate Through XAD-8 Adsorption. Procedia Environmental Sciences, 2012, 16, 3-8.	1.3	6

#	Article	IF	CITATIONS
145	In-situ emission characteristics of odorous gases from two food waste processing plants. Journal of Material Cycles and Waste Management, 2013, 15, 510-515.	1.6	6
146	Morphology characteristics and mode of CaO encapsulation during treatment of electrolytic manganese solid waste. Environmental Science and Pollution Research, 2016, 23, 21861-21871.	2.7	6
147	Mercaptopropionic acid-capped Mn-doped ZnS quantum dots and Pb2+ as sensing system for rapid and sensitive room-temperature phosphorescence detection of sulfide in water. Journal of Photochemistry and Photobiology A: Chemistry, 2018, 364, 88-96.	2.0	6
148	One-dimensional assembly of TiO ₂ nanoparticles toward enhancing light harvesting and electron transport for application in dye-sensitized solar cells. RSC Advances, 2014, 4, 10519-10524.	1.7	5
149	Concentration Quantification of Oil Samples by Three-Dimensional Concentration-Emission Matrix (CEM) Spectroscopy. Applied Sciences (Switzerland), 2020, 10, 315.	1.3	5
150	Synthesis of zero-valent iron/biochar by carbothermal reduction from wood waste and iron mud for removing rhodamine B. Environmental Science and Pollution Research, 2021, 28, 48556-48568.	2.7	5
151	Development of a Laser Gas Analyzer for Fast CO2 and H2O Flux Measurements Utilizing Derivative Absorption Spectroscopy at a 100 Hz Data Rate. Sensors, 2021, 21, 3392.	2.1	5
152	Facile one-step synthesis and enhanced photocatalytic activity of a WC/ferroelectric nanocomposite. Journal of Materials Chemistry A, 2021, 9, 22861-22870.	5.2	5
153	Simultaneous detection of heavy metals in solutions by electrodeposition assisted laser induced breakdown spectroscopy. Journal of Laser Applications, 2022, 34, 012021.	0.8	5
154	Studies on structural and mechanical properties under isostatic compression with large-scale discrete element simulations. Acta Mechanica Solida Sinica, 2014, 27, 129-136.	1.0	4
155	Sediment provenance in the western Pacific warm pool from the last glacial maximum to the early Holocene: Implications for ocean circulation and climatic change. Palaeogeography, Palaeoclimatology, Palaeoecology, 2018, 493, 55-63.	1.0	4
156	Development and Application of HECORA Cloud Retrieval Algorithm Based On the O2-O2 477 nm Absorption Band. Remote Sensing, 2020, 12, 3039.	1.8	4
157	The BioChemical Clogging of Landfill Leachate Collection System: Based on Laboratory Studies. International Journal of Environmental Research and Public Health, 2020, 17, 2299.	1.2	4
158	Formation and Mechanism of Magnesium Titanate in the Process of Ilmenite Reduction. Mineral Processing and Extractive Metallurgy Review, 2021, 42, 162-171.	2.6	4
159	Pyrolysis behaviors of oil sludge based on TG/FTIR and PY-GC/MS. Frontiers of Environmental Science and Engineering in China, 2010, 4, 59-64.	0.8	3
160	Realâ€ŧime in situ monitoring of poly(lactide―co â€glycolide) coating of coronary stents using electrochemical impedance spectroscopy. Journal of Biomedical Materials Research - Part B Applied Biomaterials, 2015, 103, 691-699.	1.6	3
161	Characterization and solidification/stabilization of iron-ore sintering gas cleaning residue. Journal of Material Cycles and Waste Management, 2015, 17, 790-797.	1.6	3
162	Industrial SO ₂ emission monitoring through a portable multichannel gas analyzer with an optimized retrieval algorithm. Atmospheric Measurement Techniques, 2016, 9, 1167-1180.	1.2	3

#	Article	IF	CITATIONS
163	Feature issue introduction: light, energy and the environment, 2017. Optics Express, 2018, 26, A636.	1.7	3
164	Contribution of continuously stable sediment input to the formation of the Pearl River delta since the middle Holocene. Quaternary International, 2021, 598, 78-89.	0.7	3
165	Novel application of pyrolytic carbon generated from waste tires: Hydrolytic and methanogenic performance promotion in vinegar residue anaerobic digestion. Waste Management, 2022, 143, 15-22.	3.7	3
166	Three-dimensional reconstruction of a leaking gas cloud based on two scanning FTIR remote-sensing imaging systems. Optics Express, 2022, 30, 25581.	1.7	3
167	Ozone Profiles, Precursors, and Vertical Distribution in Urban Lhasa, Tibetan Plateau. Remote Sensing, 2022, 14, 2533.	1.8	3
168	Correlation study between suspended particulate matter and DOAS data. Advances in Atmospheric Sciences, 2006, 23, 461-467.	1.9	2
169	Spatial and temporal variability of odorous VOC in a food waste treatment plant using hydrothermal hydrolysis and aerobic fermentation technology. Journal of Material Cycles and Waste Management, 2015, 17, 626-636.	1.6	2
170	Ecoâ€environmental benefits analysis of EcoPartnerships program of production technology of calcium carbonate from lime mud produced by alkaline papermaking. Environmental Progress and Sustainable Energy, 2021, 40, e13697.	1.3	2
171	An active RH-controlled dry-ambient aerosol size spectrometer (DAASS) for the accurate measurement of ambient aerosol water content. Journal of Aerosol Science, 2021, 158, 105831.	1.8	2
172	Technical note: Real-time diagnosis of the hygroscopic growth micro-dynamics of nanoparticles with Fourier transform infrared spectroscopy. Atmospheric Chemistry and Physics, 2022, 22, 3097-3109.	1.9	2
173	CEMENT/ACTIVATED-CARBON SOLIDIFICATION/STABILIZATION TREATMENT OF NITROBENZENET. , 2009, , .		0
174	Concentration-Emission Matrix (CEM) Spectroscopy Combined with GA-SVM: An Analytical Method to Recognize Oil Species in Marine. Molecules, 2020, 25, 5124.	1.7	0
175	Development and Application of a Wide Dynamic Range and High Resolution Atmospheric Aerosol Water-Based Supersaturation Condensation Growth Measurement System. Atmosphere, 2021, 12, 558.	1.0	0